Vortex Nucleation in Bose-Einstein Condensates in an Oblate, Purely Magnetic Potential

E. Hodby, G. Hechenblaikner, S. A. Hopkins, O. M. Maragò, and C. J. Foot

Clarendon Laboratory, Department of Physics, University of Oxford, Parks Road, Oxford, OX1 3PU, United Kingdom

(Received 13 June 2001; published 19 December 2001)

We have investigated the formation of vortices by rotating the purely magnetic potential confining a Bose-Einstein condensate. We modified the bias field of an axially symmetric TOP trap to create an elliptical potential that rotates in the radial plane. This enabled us to study the conditions for vortex nucleation over a wide range of eccentricities and rotation rates.

DOI: 10.1103/PhysRevLett.88.010405 PACS numbers: 03.75.Fi, 32.80.Pj, 67.90.+z

The existence of quantized vortices is one of the most striking and fascinating signatures of superfluidity. There has been theoretical interest in vortices in a dilute gas Bose-Einstein condensate for many years (for a review see, for example, [1]) and the recent experimental observations [2,3] have stimulated much further work. Vortices have been nucleated using phase imprinting [2] and by using a laser beam "stirrer" [3,4]. We have used a new, purely magnetic excitation scheme, which like the optical stirrer has a close analogy to the "rotating bucket" experiment with liquid He [5]. Vortices provide dramatic visual evidence for the single condensate wave function. Furthermore, the detailed mechanisms for the formation, stabilization, and decay of vortices reveal new information about the dynamics of the excited states of the condensate and its interaction with the thermal cloud. The excited states and hence the conditions for nucleation depend on the geometry of the confining potential [6]. Our work in an oblate geometry compliments the work done to date in prolate and spherical traps. The range of eccentricity available in our purely magnetic rotating trap [7] is much greater than in previous experiments, where the radial symmetry was broken by "stirring" the condensate with the dipole force from off-resonant laser beams.

We have measured the relationship between the eccentricity of the trap in the plane of rotation and the angular frequency Ω that must be satisfied to nucleate vortices in our trap. The trap has a harmonic potential with oscillator frequencies $\omega_x < \omega_y < \omega_z$. The shape of the trap is characterized by the deformation parameter ϵ, given by

$$\epsilon = \frac{\omega_y^2 - \omega_x^2}{\omega_x^2 + \omega_y^2}. \quad (1)$$

We show that when the trap is adiabatically ramped from circular, $\epsilon = 0$, to a given eccentricity, there is both an upper and lower critical rotation rate for nucleation. We present the threshold conditions for vortex nucleation in our geometry and finally discuss the role of the thermal cloud in both the nucleation and stabilization processes.

A detailed description of the rotating elliptical trap is given in [7] and only a summary of the technique is presented here. Our time-averaged orbiting potential (TOP) trap consists of a spherical quadrupole field and a rapidly rotating bias field [8]. The zero of the magnetic field describes a circle in the radial (XY) plane. The atoms experience a time-averaged, axially symmetric harmonic potential. If the X and Y components of the bias field (B_x and B_y) are not of equal amplitude, then the axial symmetry is broken and the potential becomes elliptical in the XY plane. The ratio of the radial trap frequencies ω_x/ω_y can be calculated numerically from B_y/B_x. For small eccentricities $\omega_x/\omega_y - 1 \approx (B_y/B_x - 1)/4$. To rotate the elliptical potential we modulated B_x and B_y at Ω, a frequency much lower than the TOP frequency ω_0. The final bias field has the form of a rotation matrix through angle Ωt multiplying the X and Y components of an ellipse:

$$\begin{pmatrix} B_x \\ B_y \end{pmatrix} = \begin{pmatrix} \cos\Omega t & \sin\Omega t \\ -\sin\Omega t & \cos\Omega t \end{pmatrix} \begin{pmatrix} EB_t \cos\omega_0 t \\ B_t \sin\omega_0 t \end{pmatrix}. \quad (2)$$

During any particular evaporative cooling run, the value of Ω, the angular frequency at which the elliptical trap rotates, was fixed (for technical reasons), and so the trap was always rotating. To create a "static" trap for efficient evaporative cooling, the bias field ratio, E, is set to 1 so that the trap is symmetric around the rotation axis. This symmetry was checked to be accurate to $\epsilon = 0 \pm 0.005$ using measurements of the frequency of dipole oscillations in the X and Y directions. Evaporative cooling in the static trap, followed by an adiabatic expansion, resulted in a condensate of 2×10^4 atoms, at a temperature of $0.5T_c$. At this stage the trap is axially symmetric, $\omega_x = \omega_y$, with trap frequencies typically $\omega_x/2\pi = 62$ Hz and $\omega_z/2\pi = 175$ Hz.

Then to create vortices, the value of E was ramped linearly over 200 ms from 1 to its final value, to give a trap that was elliptical and rotating. When we create an eccentric trap by increasing (decreasing) the TOP bias field, all three trap frequencies are reduced (increased). Since vortex lifetimes depend on the mean trap frequency [9], we adjusted the quadrupole field in the adiabatic expansion stage, to ensure that all traps had the same average radial trap frequency $\omega_\perp$, defined as

$$\omega_\perp = \sqrt{\frac{\omega_x^2 + \omega_y^2}{2}}. \quad (3)$$

The condensate was then held in the rotating anisotropic trap [7] for a further 800 ms before being released. After 12 ms of free expansion the cloud was imaged along the

axis of rotation using an absorption imaging system with 3 μm resolution. Figure 1 shows images of the expanded condensate at different stages during the nucleation process. Initially the cloud elongates, confirming that nucleation is being mediated by excitation of a quadrupole mode [Fig. 1(a)] [10]. Then fingerlike structures appear on the outside edge of the condensate which eventually close round and produce vortices ~800 ms after rotation began [Fig. 1(b)]. Approximately 200 ms later, these have moved to equilibrium positions within the bulk of the condensate. Figures 1(c) and 1(d) show typical, single-shot images of stable vortex arrangements. The depth of each vortex (in the integrated absorption profile) is approximately 95% of the surrounding condensate. The core diameters of ~5 μm after 12 ms of free expansion are consistent with the predictions in [11]. The maximum number of vortices we observed was seven, limited by the number of atoms in our condensate.

Our first study of the nucleation process involved counting the number of vortices as a function of the normalized trap rotation rate, $\overline{\Omega} = \Omega/\omega_\perp$, for a fixed eccentricity. Results for trap deformations $\epsilon = 0.084$ and 0.041 are given in Fig. 2. These graphs show a maximum and a minimum value of $\overline{\Omega}$ for nucleation at a given eccentricity. Increasing ϵ increases the range of $\overline{\Omega}$ over which vortices may be nucleated, both by lowering $\overline{\Omega}_{\min}$ and raising $\overline{\Omega}_{\max}$. In the limit of small eccentricities, $\sqrt{2}\,\omega_\perp$ is the frequency of the $m = 2$ quadrupole mode, which has been shown elsewhere to play a critical role in the nucleation process [10]. Rotation of the ellipsoidal trap at half this frequency, i.e., $\overline{\Omega}_c = 1/\sqrt{2} \simeq 0.71$, excites this mode. The plots in Fig. 2 confirm that the nucleation depends on resonant excitation of the quadrupole mode as seen previously [4,10]. The resonance is broader at higher eccentricity, as intuitively expected for stronger driving.

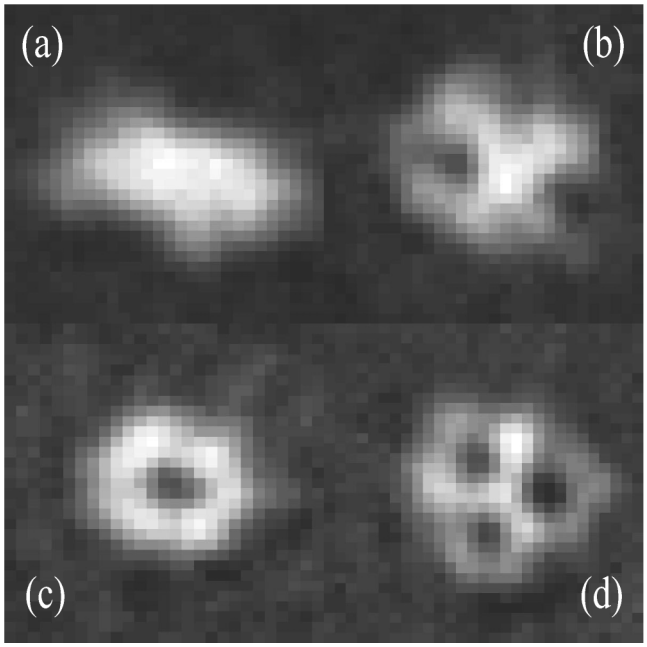

FIG. 1. Images of the condensate at different stages during the vortex nucleation process. (All taken with $\overline{\Omega} = 0.70$ and $\epsilon = 0.05$ and after 12 ms of free expansion.) (a) After the 200 ms spinning eccentricity ramp, the condensate is elongated, indicating that a quadrupole mode has been excited. (b) After a further 600 ms in the spinning trap one vortex has just formed near the edge. After 800 ms, the vortices have reached their equilibrium positions and appear in symmetrical configurations. (c) One centered vortex, typical under these conditions. (d) A triangular array of three vortices.

Our second study involved holding $\overline{\Omega}$ constant and counting the number of vortices as a function of the trap deformation ϵ. Figure 3 shows our results for two cases: (a) $\overline{\Omega} > \overline{\Omega}_c$ and (b) $\overline{\Omega} < \overline{\Omega}_c$. Interestingly, we were able to nucleate vortices under adiabatic conditions when $\overline{\Omega} < \overline{\Omega}_c$. We employ the adiabaticity criterion $\dot{\epsilon}/\epsilon \ll \omega_\perp$. As a further check of the adiabaticity we varied the time for the eccentricity ramp between 200 ms and 1 s, and detected no difference in the number of vortices formed.

The critical values of $\overline{\Omega}$ and ϵ for nucleation were extracted from plots such as Figs. 2 and 3 for many values of $\overline{\Omega}$ and compiled on Fig. 4. The data points show the minimum eccentricity required for a given rotation rate and map out region 2, within which vortices nucleate. $\overline{\Omega}_c$ appears to be a critical rotation frequency at which vortices can be nucleated with minimum eccentricity, as predicted in [12]. Changing $\overline{\Omega}$ from 0.71 in either direction requires a more elliptical trap for nucleation, although different physical processes control the upper and lower limits as explained below.

At $\overline{\Omega} > \overline{\Omega}_c$, the condensate follows a particular quadrupole mode at small eccentricity, region 3 in Fig. 4. This mode is referred to as the "overcritical branch" in [13], and we have observed that it has an elliptical density

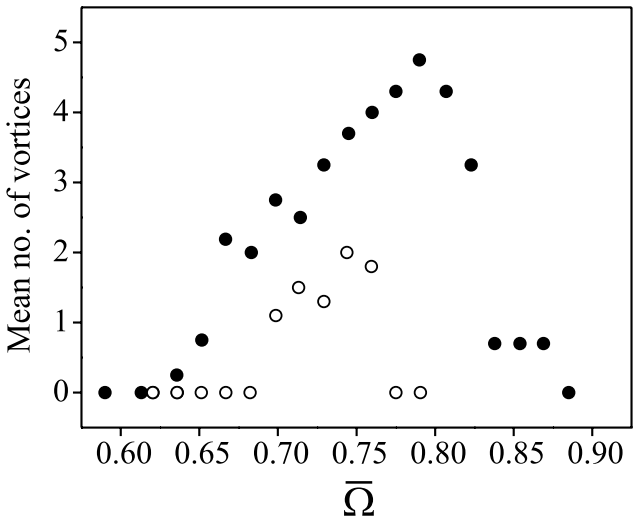

FIG. 2. The mean number of vortices as a function of the normalized trap rotation rate $\overline{\Omega} = \Omega/\omega_\perp$. Two different trap eccentricities were used, $\epsilon = 0.041$ (open circles) and $\epsilon = 0.084$ (solid circles). Each data point is the mean of four runs.

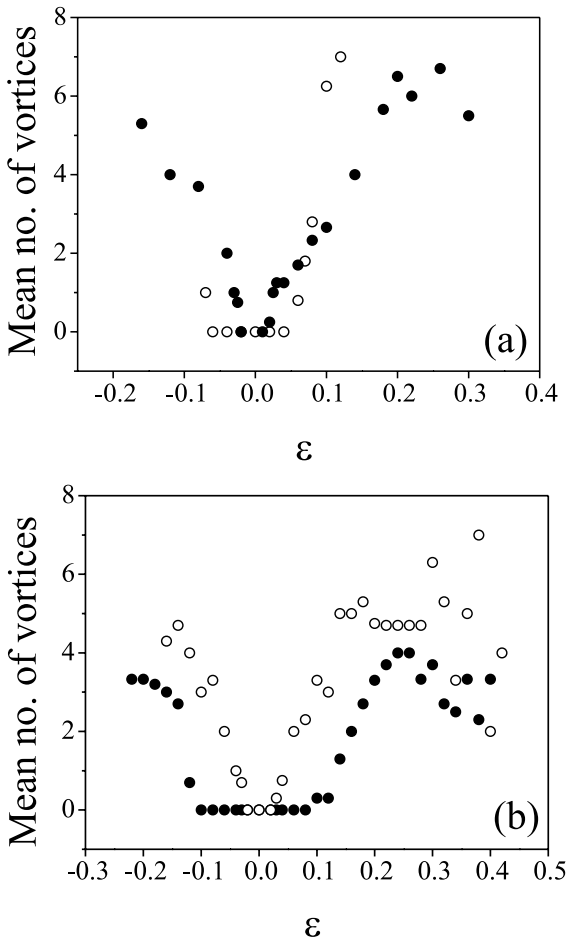

FIG. 3. The mean number of vortices as a function of trap deformation at four different trap rotation rates: (a) above and (b) below the critical value $\overline{\Omega}_c = 0.71$. In (a), $\overline{\Omega} = 0.74$ (solid circles) and 0.81 (open circles). In (b) $\overline{\Omega} = 0.61$ (solid circles) and 0.70 (open circles). Positive (negative) ϵ corresponds to $\omega_x < \omega_y$ ($\omega_x > \omega_y$).

distribution which is orthogonal to the trap potential, as predicted by numerical simulations [14]. It then nucleates vortices when the eccentricity is too large for the quadrupole mode to be a solution of the hydrodynamic equations. The boundary of the region in the ϵ versus $\overline{\Omega}$ plot where this quadrupole mode exists is given by

$$\epsilon = \frac{2}{\overline{\Omega}}\left(\frac{2\overline{\Omega}^2 - 1}{3}\right)^{3/2}. \quad (4)$$

We determined this relation from the solutions of the hydrodynamic equations for superfluids, and it is plotted as a solid line in Fig. 4. This line agrees well with the experimental data for the critical conditions for nucleation for $\overline{\Omega} > \overline{\Omega}_c$ and a wide range of ϵ.

Below $\overline{\Omega}_c$, the deformation needed to nucleate vortices appears to increase linearly with $\overline{\Omega}$. This boundary cannot be explained in terms of the stability limit of a quadrupole mode—the "normal branch" is stable on both regions 1 and 2 and the overcritical branch is stable in neither. Our data appear to be at variance with the results in [10], where

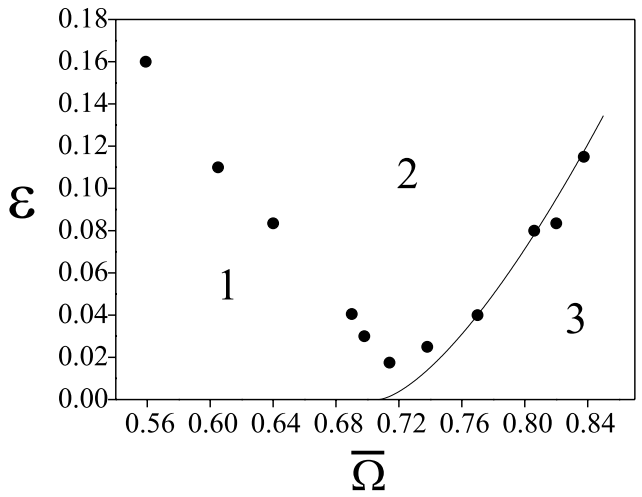

FIG. 4. The critical conditions for vortex nucleation. The data points mark the minimum trap deformation for nucleation at a particular $\overline{\Omega}$. Vortices may be formed in region 2. The solid line shows the theoretical limit of stability of the quadrupole mode, which is stable in region 3. This line is in good agreement with the extreme conditions for vortex formation at $\overline{\Omega} > \overline{\Omega}_c$

no vortices were seen when the eccentricity was increased adiabatically and $\overline{\Omega} < \overline{\Omega}_c$. We have observed that on this branch the elliptical density distribution is parallel to the trap potential, again in agreement with [14].

A mechanism for the creation of vortices at a frequency below $\overline{\Omega}_c$ has been proposed in [12]. They have shown that there are regions in the plot of ϵ versus $\overline{\Omega}$, both above and below $\overline{\Omega}_c$, where the quadrupole solutions of the hydrodynamic equations become dynamically unstable. For frequencies above $\overline{\Omega}_c$ the predicted instability domains coincide with the experimentally observed vortex domains in [10] and this work, thus indicating a link between their instability analysis and vortices. To make a quantitative prediction for the boundary between regions 1 and 2 shown in Fig. 4 will require further detailed work for our specific case. We also note that it is possible that there exist non-negligible terms of higher order than quadratic in the rotating magnetic potential. These have been demonstrated to excite high order rotating surface modes, e.g., hexapole, which lead to vortex nucleation at frequencies less than $\overline{\Omega}_c$ [4,10].

Another possible mechanism for observation of vortices below $\overline{\Omega}_c$ is that the thermal cloud plays an important role. Transfer of angular momentum to the condensate from the spinning thermal cloud may provide a mechanism for vortices to form at $\overline{\Omega} < \overline{\Omega}_c$. However, the transfer rate of angular momentum must be greater than any loss rate due to residual trap anisotropy [15]. In [10], gravity produces a small static eccentricity in the trap in the plane of rotation. The "spin down" time for a rotating thermal cloud in the presence of a deformation parameter ϵ of only 0.01 is very short, 0.5 s, compared to the spin up time of 15 s, and hence the cloud may never gain significant angular momentum. However, in our experiment, gravity

acts along the rotation axis and hence the trap is symmetric in the plane of rotation, giving a more favorable ratio of spin up to spin down times.

With this hypothesis in mind, we tested our nucleation curve at lower temperature to see if there was any change when the amount of thermal cloud was reduced. When acquiring the data of Fig. 4 the rf was turned off after condensation and some heating was observed during the nucleation procedure, resulting in a temperature around $0.8T_c$. To achieve a lower temperature we left on the so-called "rf shield" so as to give an effective trap depth of 800 nK during the nucleation process. This resulted in a temperature of $0.5T_c$. No significant change was observed in the nucleation curve at this lower temperature. However, this does not totally rule out a role for the thermal cloud in the nucleation process in our experiment since even at $0.5T_c$, there was still a significant 20% of atoms in the thermal cloud.

Although the exact amount of thermal cloud seemed to have little effect on the nucleation conditions, it had a striking effect on the behavior of vortices after nucleation. Without the rf shield during the nucleation process, vortices were only occasionally found in an equilibrium configuration (i.e., 1 vortex in the center, 3 vortices in an equilateral triangle as in Fig. 1), and $\sim$400 ms after forming they had already moved to the edge of the condensate before disappearing. However, with the rf shield present, the vortices were normally found in equilibrium positions $\sim$200 ms after formation and had a lifetime of $\sim$4 s, limited only by the decay of the condensate itself.

In summary, we have used a purely magnetic rotating trap to investigate conditions for vortex nucleation (after the formation of the condensate) over a wide range of trap eccentricities. For a given eccentricity, we observe both an upper and a lower limit to the rotation rate for nucleation. The upper limit confirms the predictions in [10], but over a much wider range of parameters. However, the lower limit to the rotation rate is different from that reported elsewhere. Further theoretical work is required to explain the linear dependence of ϵ on $\overline{\Omega}$ shown in Fig. 4. The thermal cloud is shown to destabilize vortex arrays, thus measurements of the vortex lifetime in an oblate geometry were made with an rf shield to prevent heating.

The rotating anisotropic magnetic trap offers several advantages, including the absence of spontaneous emission losses as incurred with dipole force stirrers, ease of alignment and adjustment, and enabling the production of large eccentricities. It has recently been used to investigate the irrotational behavior of vortex-free condensates at low rotation rates [16]. A large eccentricity is also needed to spin up a thermal cloud [15]; hence this trap may be useful in attempts to condense directly into a vortex state from a spinning thermal cloud in thermodynamic equilibrium.

We thank D. Feder for his numerical simulations of our trap and J. Arlt for his part in constructing the experiment. This work was supported by the EPSRC and the TMR program (No. ERB FMRX-CT96-0002). O. M. M. acknowledges the support of a Marie Curie Fellowship, TMR program (No. ERB FMBI-CT98-3077).

Note added.— Under different conditions, the thermal cloud has been shown to play an essential role in vortex formation [17].

[1] A. Fetter and A. Svidzinsky, J. Phys. Condens. Matter **13**, R135 (2001).
[2] M. R. Matthews, B. P. Anderson, P. C. Haljan, D. S. Hall, C. E. Wieman, and E. A. Cornell, Phys. Rev. Lett. **83**, 2498 (1999).
[3] K. W. Madison, F. Chevy, W. Wohlleben, and J. Dalibard, Phys. Rev. Lett. **84**, 806 (2000).
[4] J. R. Abo-Shaeer, C. Raman, J. M. Vogels, and W. Ketterle, Science **292**, 476 (2001).
[5] R. J. Donnelly, *Quantised Vortices in Helium II* (Cambridge University Press, Cambridge, U.K., 1991).
[6] F. Dalfovo and S. Stringari, Phys. Rev. A **63**, 011601(R) (2001); D. Feder *et al.,* Phys. Rev. Lett. **82**, 4956 (1999); J. Garcia-Ripoll and V. Perez-Garcia, Phys. Rev. A **64**, 013602 (2001).
[7] J. Arlt, O. M. Maragò, E. Hodby, S. A. Hopkins, G. Hechenblaikner, S. Webster, and C. J. Foot, J. Phys. B **32**, 5861 (1999).
[8] W. Petrich, M. Anderson, J. Ensher, and E. A. Cornell, Phys. Rev. Lett. **74**, 3352 (1995).
[9] P. Fedichev and G. Shlyapnikov, Phys. Rev. A **60**, R1779 (1999).
[10] K. W. Madison, F. Chevy, V. Bretin, and J. Dalibard, Phys. Rev. Lett. **86**, 4443 (2001); F. Chevy, K. W. Madison, V. Bretin, and J. Dalibard, cond-mat/0104218.
[11] E. Lundh, C. J. Pethick, and H. Smith, Phys. Rev. A **58**, 4816 (1998).
[12] S. Sinha and Y. Castin, cond-mat/0101292.
[13] A. Recati, F. Zambelli, and S. Stringari, Phys. Rev. Lett. **86**, 377 (2001).
[14] D. Feder (private communication).
[15] D. Guery-Odelin, Phys. Rev. A **62**, 033607 (2000).
[16] G. Hechenblaikner, E. Hodby, S. A. Hopkins, O. M. Maragò, and C. J. Foot, cond-mat/0106182.
[17] P. C. Haljan, I. Coddington, P. Engels, and E. A. Cornell, cond-mat/0106362.